

## DETECTION OF WIDESPREAD HYDRATED MATERIALS ON VESTA BY THE VIR IMAGING SPECTROMETER ON BOARD THE DAWN MISSION

M. C. DE SANCTIS<sup>1</sup>, J.-PH. COMBE<sup>2</sup>, E. AMMANNITO<sup>1</sup>, E. PALOMBA<sup>1</sup>, A. LONGOBARDO<sup>1</sup>, T. B. MCCORD<sup>2</sup>, S. MARCHI<sup>3</sup>, F. CAPACCIONI<sup>1</sup>, M. T. CAPRIA<sup>1</sup>, D. W. MITTFELDLT<sup>4</sup>, C. M. PIETERS<sup>5</sup>, J. SUNSHINE<sup>6</sup>, F. TOSI<sup>1</sup>, F. ZAMBON<sup>1</sup>, F. CARRARO<sup>1</sup>, S. FONTE<sup>1</sup>, A. FRIGERI<sup>1</sup>, G. MAGNI<sup>1</sup>, C. A. RAYMOND<sup>7</sup>, C. T. RUSSELL<sup>8</sup>, AND D. TURRINI<sup>1</sup>

<sup>1</sup> Istituto di Astrofisica e Planetologia Spaziali, INAF, Rome, Italy; [mariacristina.desanctis@iaps.inaf.it](mailto:mariacristina.desanctis@iaps.inaf.it)

<sup>2</sup> Bear Fight Institute, Winthrop, WA, USA

<sup>3</sup> NASA Lunar Science Institute, Boulder, CO, USA

<sup>4</sup> NASA Johnson Space Center, Houston, TX, USA

<sup>5</sup> Department of Geological Sciences, Brown University, Providence, RI, USA

<sup>6</sup> Department of Astronomy, University of Maryland, Maryland, USA

<sup>7</sup> Jet Propulsion Laboratory, California Institute of Technology, Pasadena, CA, USA

<sup>8</sup> Institute of Geophysics and Planetary Physics, University of California, Los Angeles, CA, USA

Received 2012 August 17; accepted 2012 September 5; published 2012 October 3

### ABSTRACT

Water plays a key role in the evolution of terrestrial planets, and notably in the occurrence of Earth's oceans. However, the mechanism by which water has been incorporated into these bodies—including Earth—is still extensively debated. Here we report the detection of widespread 2.8  $\mu\text{m}$  OH absorption bands on the surface of the asteroid Vesta by the VIR imaging spectrometer on board *Dawn*. These observations are surprising as Vesta is fully differentiated with a basaltic surface. The 2.8  $\mu\text{m}$  OH absorption is distributed across Vesta's surface and shows areas enriched and depleted in hydrated materials. The uneven distribution of hydrated mineral phases is unexpected and indicates ancient processes that differ from those believed to be responsible for OH on other airless bodies, like the Moon. The origin of Vestan OH provides new insight into the delivery of hydrous materials in the main belt and may offer new scenarios on the delivery of hydrous minerals in the inner solar system, suggesting processes that may have played a role in the formation of terrestrial planets.

*Key words:* minor planets, asteroids: general – minor planets, asteroids: individual: (Vesta)

*Online-only material:* color figures

### 1. INTRODUCTION

Vesta is the largest fully differentiated asteroid. It has a basaltic surface dominated by a spectral signature of the mafic silicate mineral, pyroxene (McCord et al. 1970; Gaffey 1997; De Sanctis et al. 2012). Its spectra are similar to those of howardite, eucrite, and diogenite meteorites (HEDs), so it has been suggested that Vesta is the source of this class of meteorites (Consolmagno & Drake 1977; Takeda 1997; Drake 2001). A family of small, V-type asteroids, the so-called Vestoids, is dynamically associated with Vesta (Binzel & Xu 1993; Duffard et al. 2004; Moskovitz et al. 2010; De Sanctis et al. 2011a, 2011c). Notably, the link between distant Vestoids and HEDs is provided by several V-types observed among near-Earth objects (e.g., Marchi et al. 2005). HEDs formed under moderately reducing conditions and have low concentrations of volatile elements (Mittlefehldt et al. 1998). The HED parent body is thought to be volatile-depleted, as evidence for hydrous alteration is rarely found in HEDs (Mittlefehldt & Lindstrom 1997; Treiman et al. 2004; Barrat et al. 2011). Apatite, a volatile-bearing mineral, is a minor constituent of eucrites and very rare in diogenites.

Carbonaceous chondritic clasts are frequently found in howardites (Zolensky et al. 1996; Gounelle et al. 2003) and exhibit varying degrees of aqueous alteration. These chondritic clasts can contain H<sub>2</sub>O in the form of hydrated, hydroxylated, or oxyhydroxylated mineral phases. A weak hydration signature in the 3  $\mu\text{m}$  region has been reported for Vesta from telescopic data, but this discovery has not been independently confirmed (Rivkin et al. 2006; Hasegawa et al. 2003).

VIR, the imaging spectrometer on board the *Dawn* spacecraft (De Sanctis et al. 2011b; Russell et al. 2012), provides high-quality spectra of Vesta in the 0.25–5.1  $\mu\text{m}$  range, and thus has the capability of detecting absorptions caused by hydrated phases. We have analyzed the 3  $\mu\text{m}$  spectral region to search for evidence of hydration, and this Letter reports on the absorption due to OH (hydroxyl) near 2.8  $\mu\text{m}$ .

### 2. DATA ANALYSES

VIR is a high-resolution imaging spectrometer with a spatial sampling of 250  $\mu\text{rad}$ . It combines two sets of focal planes and detectors in one compact instrument: the visible detector covers the spectral range 0.25–1.07  $\mu\text{m}$ , and the infrared covers the 0.95–5.1  $\mu\text{m}$  range, with a spectral sampling of  $\Delta\lambda_{\text{VIS}} = 1.8 \text{ nm band}^{-1}$  and  $\Delta\lambda_{\text{IR}} = 9.8 \text{ nm band}^{-1}$ , respectively.

In this analysis, we focus on the data obtained during the approach and survey phases (Russell & Raymond 2011) with a nominal spatial sampling varying from 1.3 to  $\sim 0.7$  km due to the different orbital altitudes. The orientation of Vesta's spin axis and *Dawn*'s orbital characteristics in these orbits has allowed about 65% of the surface to be imaged, ranging from the south pole up to about 40° north latitude. During these two orbital phases, VIR acquired spectra under different illumination conditions, local hours, and spatial resolutions, with phase angles from 67°8 to 7°9.

Initially, by using the first ground-derived response function, VIR data in the spectral domain near the short wavelength edge of the OH–H<sub>2</sub>O region were affected by incomplete calibration (De Sanctis et al. 2012). However, no artifacts are visible in

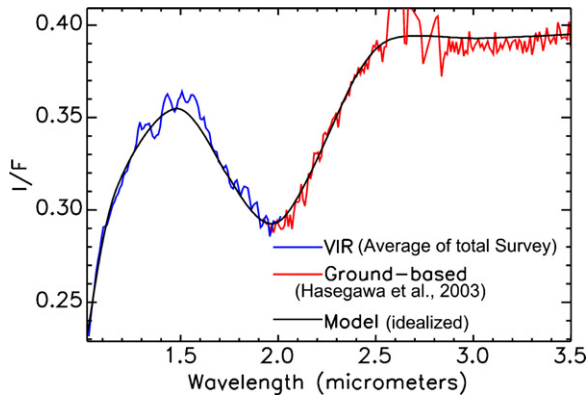


**Figure 1.** Calibration response function correction of the infrared detector of VIR. The average  $I/F$  spectrum of Vesta from the VIR Survey (blue) is used between 1 and 2  $\mu\text{m}$ . Telescopic observations by Hasegawa et al. (2003; red) are scaled to the VIR average spectrum. An idealized model (black) is obtained by smoothing and linear interpolation.

(A color version of this figure is available in the online journal.)

the 2.4–3.0  $\mu\text{m}$  range on ratioed spectra, indicating that the instrument is responding linearly. Thus, a simple correction of the response function based on an empirical calibration correction is appropriate to recover the signal in that specific range. We calculated the average of the spectra by Hasegawa et al. (2003), and we scaled them to the average spectrum of VIR in the hydration bands range. Then, we calculated an idealized smooth spectrum in order to eliminate the noise. This calculation was made by linear interpolation, assuming no absorption band in the 2.4–3.0  $\mu\text{m}$  wavelength range (Figure 1). Finally, the ratio between the model and the measurement is used for the correction as a multiplier to each VIR spectrum.

The newly calibrated data have been filtered for incidence angles (the angle between the incident ray and the normal)  $< 80^\circ$  and only spectra from south of  $30^\circ\text{N}$  latitude have been analyzed for absorption signatures in the 2.8–3.0  $\mu\text{m}$  range to eliminate residual effects of very poor illumination conditions in the northern hemisphere.

For spectral analysis, radiance data are converted to apparent reflectance  $I/F$  which includes (1) a normalization to the solar flux and (2) a correction of the illumination and observation geometry assuming the Lommel–Seeliger theory,

$$I/F = \pi d^2 / F \times [\cos(e) + \cos(i)] / \cos(i),$$

where  $I$  is the radiance measured in  $\text{W m}^{-2} \text{sr}^{-1} \mu\text{m}^{-1}$ ,  $F$  is the solar flux (solar spectrum) at 1 astronomical unit (AU) in  $\text{W m}^{-2} \mu\text{m}^{-1}$ ,  $d$  is the distance from the Sun to Vesta in AU, and  $i$  and  $e$  are the incidence and emergence angles, respectively.

### 3. RESULTS

An absorption at 2.8  $\mu\text{m}$  is clearly evident in VIR data for some areas on Vesta (Figure 2). Its detection is spatially coherent and repeatable in observations of the same region taken from different orbital phases, implying that the detection is linked directly to Vesta’s surface properties. Assuming the global average spectrum of Vesta has constant reflectance between 2.6 and 3  $\mu\text{m}$ , the relative 2.8  $\mu\text{m}$  band depth varies with a maximum value of the absorption of 4%. The weak 2.8  $\mu\text{m}$  feature (Figures 2(c) and (d)), and perhaps a secondary feature between 3.0–3.1  $\mu\text{m}$ , appears smooth and does not exhibit the sharp absorption common to phyllosilicates. Numerous attempts to

characterize 2.8  $\mu\text{m}$  band in extraterrestrial materials have been done recently (Hiroi et al. 1996; Sato et al. 1997; Cloutis et al. 2011). Laboratory spectra are taken under careful “dry” conditions to avoid terrestrial water contamination. Nevertheless, almost all carbonaceous chondrites samples bear significant terrestrial weathering and/or adsorbed hydration, so direct comparison between Vesta 2.8  $\mu\text{m}$  features and laboratory data is extremely difficult.

A large portion of Vesta’s surface contains the 2.8  $\mu\text{m}$  signature but its distribution is uneven (Figure 3). There are areas that are relatively enriched in OH and others that lack OH. Large regional concentrations of OH and several localized concentrations, clearly associated with observed geological features, are mapped with VIR data. The strongest absorptions of hydrated materials occur in a very large region between  $70^\circ\text{E}$  to  $220^\circ\text{E}$  and  $30^\circ\text{N}$  to  $30^\circ\text{S}$  (OH-Rich Terrain 1, OHRT1). The extent of OHRT1 is outlined in Figure 3. Because of the poor illumination conditions of the northern hemisphere, OHRT1 may extend farther north than currently mapped. This region is interrupted by an area with a weak OH-absorption band, which corresponds to the young Marcia crater ( $190^\circ\text{E}$ ,  $10^\circ\text{N}$ ). OHRT1 is found to have the highest H regional concentration by the Dawn Gamma Ray and Neutron Detector (GRaND; Prettyman et al. 2012). Another isolated region with a strong OH-absorption band, but much smaller in extent, corresponds to the crater Oppia and its ejecta (OHRT2, in Figure 3). Both of these regions lie outside the Rheasilvia basin, which lacks a 2.8  $\mu\text{m}$  signature, suggesting a relative depletion in hydrated materials. GRaND also shows that the Rheasilvia basin has the lowest average H concentrations (Prettyman et al. 2012).

The 2.8  $\mu\text{m}$  signatures are often associated with low albedo areas (Figure 4). When OH is associated with dark materials, band depths increase with decreasing albedo (Figure 2), indicating that dark material is plausibly responsible for OH signatures. However, the hydrated OH signature is also observed in some areas where dark deposits are not clearly visible, such as in the vicinity of the Oppia crater (OHRT2). The Oppia crater is associated with broad, spectrally distinct ejecta and shows large spectral variations within the crater walls and floor (De Sanctis et al. 2012).

VIR data indicate that a minor hydrated phase or hydration process occurred on Vesta’s surface. This result suggests that Vesta contains hydrated mineral phases that might be endogenic to Vesta or could have been supplied by OH-bearing impactors. Alternatively, OH might also be continuously created by interaction of solar-wind protons with the surface, forming superficial OH bonds, as has been found for the Moon (Pieters et al. 2009; Sunshine et al. 2009; McCord et al. 2011).

### 4. DISCUSSION AND CONCLUSIONS

Previous ground-based observations reported different results on the presence of 2.8  $\mu\text{m}$  band on Vesta. Hasegawa et al. (2003) reported hydrated and/or hydroxylated minerals on the surface of part of the high albedo hemisphere of Vesta. Rivkin et al. (2006) reported a small north to south increase in the 2.95/2.20  $\mu\text{m}$  band ratio, suggesting possible changes in the 3  $\mu\text{m}$  band depths. However, they also reported that “their data do not support the finding that there are hydrated minerals on Vesta”. Thus, the ground-based observations of Vesta in the spectral region where OH bands might occur are ambiguous.

The observed relative 2.8  $\mu\text{m}$  band depth distribution mapped on Vesta by VIR is very different from what is observed on the Moon. On the Moon, the measured absorption depths of OH

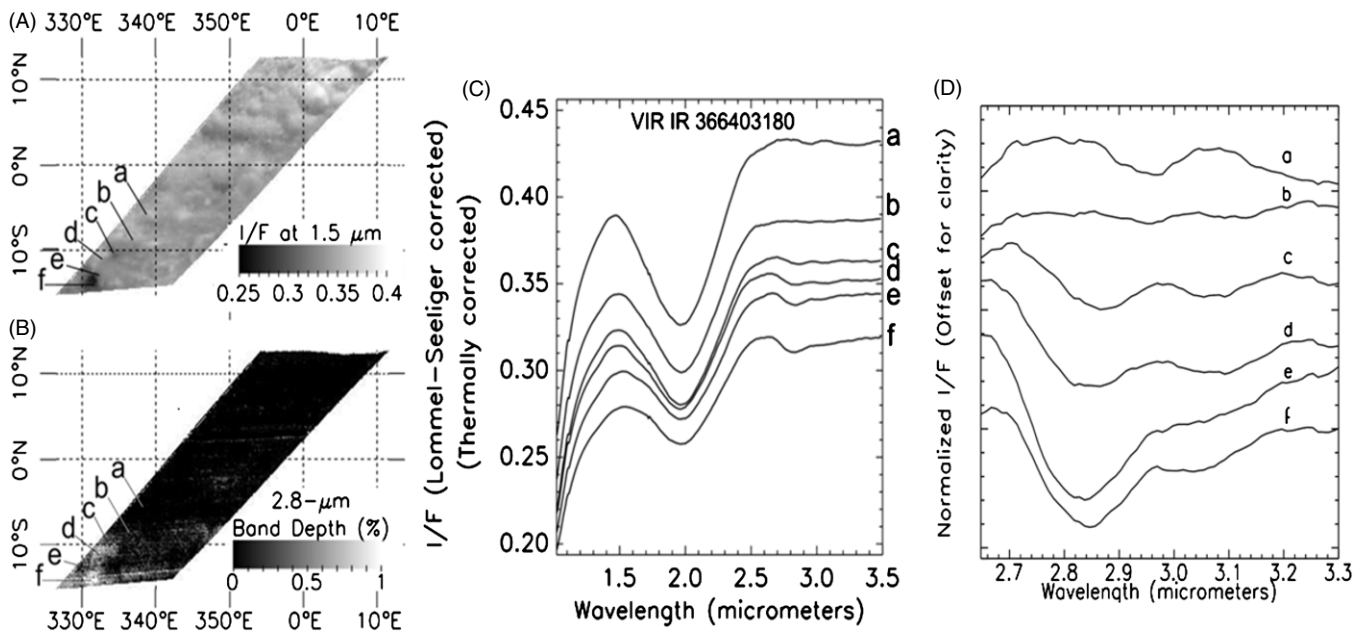


**Figure 2.** Portion of Vesta surface acquired by VIR during the Survey orbits. (A)  $I/F$  at  $1.5 \mu\text{m}$ . (B) Map of the  $2.8 \mu\text{m}$  band depth of the same region. (C) Reflectance spectra from the different locations labeled in (A) and (B), showing increasing  $2.8 \mu\text{m}$  band depths going from “a” to “f”. (D) The same as (C) but enlarged to show the  $2.8 \mu\text{m}$  shape better.

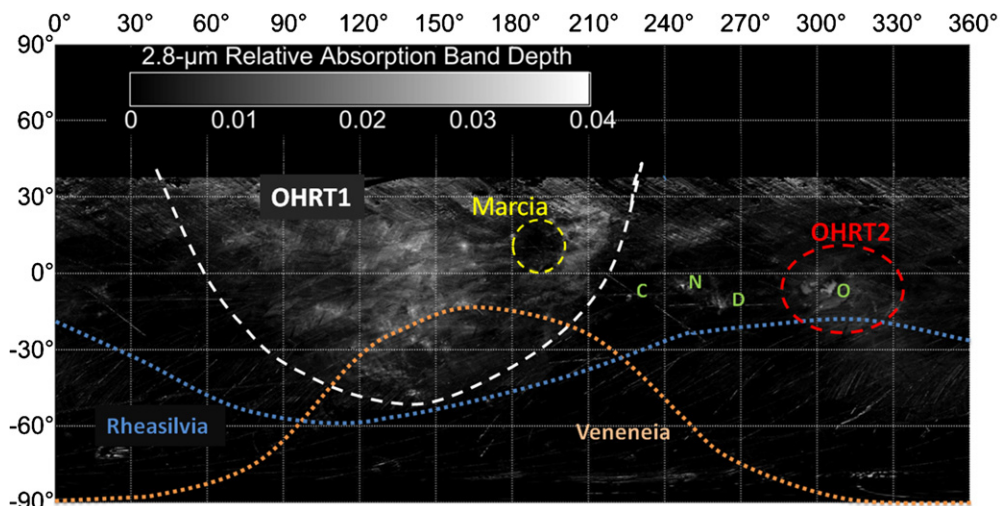


**Figure 3.**  $2.8 \mu\text{m}$  band distribution on Vesta surface. The boundaries of two large impact basins (Rehasilvia and Veneneia) and the Marcia crater are shown with the OH-Rich-Regions 1 (OHRT1) and 2 (OHRT2). C, N, D, and O are, respectively, the Cornelia, Numisia, Drusilia, and Oppia craters.

(A color version of this figure is available in the online journal.)

and/or  $\text{H}_2\text{O}$  increase dramatically with latitude beyond  $45^\circ$  and appear to vary as a function of the local time of day (Pieters et al. 2009; Sunshine et al. 2009; McCord et al. 2011). Because of that OH and/or  $\text{H}_2\text{O}$  are mainly attributed to solar-wind protons that interact with the lunar surface, forming surficial O-H bonds that are highly dependent on the temperature and solar illumination environment. On Vesta, there are no significant correlations of the  $2.8 \mu\text{m}$  band depth with illumination or temperature, which is also retrieved by VIR in the thermal wavelength region. Moreover, because the temperature of the surface of Vesta is  $\leq 273 \text{ K}$ , thermal emission does not affect the absorption band depth at  $2.8 \mu\text{m}$  and the analysis is therefore not affected by possible problems related to the removal of thermal emission. Furthermore, the Vesta OH spatial distribution is stable over time. The temporally constant longitudinal variation in  $2.8 \mu\text{m}$  band depth on Vesta (Figure 3) contrasts with the temporally

and latitudinally variable distribution seen on the Moon that has been used to point to a solar-wind origin (Pieters et al. 2009; Sunshine et al. 2009; McCord et al. 2011). This suggests that the origin of OH on Vesta is not due to short-term surface processes, nor to those that require significant shadowing or unusual cold temperatures.

The distribution of the hydration band on Vesta is more likely related to other factors such as differences in the mineralogy of Vestan materials and/or the presence of exogenous OH-bearing materials. The plot of the  $1.9 \mu\text{m}$  band centers versus  $2.8 \mu\text{m}$  band depths (Figure 4(b)) indicates that the stronger OH signature is associated with howarditic and eucritic material, i.e., stronger  $2.8 \mu\text{m}$  absorptions are found in regions where  $1.9 \mu\text{m}$  band centers are shifted toward longer wavelengths as observed for eucrite-rich howardites (De Sanctis et al. 2012). Nevertheless, we have also found regions of rich

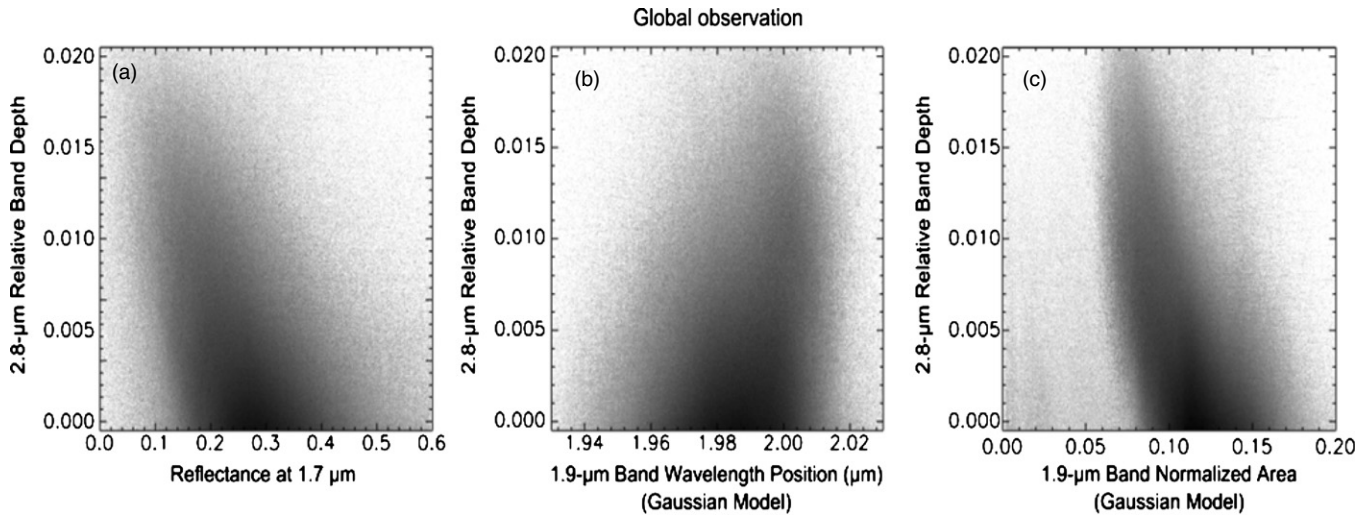


**Figure 4.** Scatter plot from VIR observations as in Figure 2, showing the correlation between 2.8  $\mu\text{m}$  absorption band depths and other spectral parameters (reflectance at 1.7  $\mu\text{m}$ , 1.9  $\mu\text{m}$  band centers, and 1.9  $\mu\text{m}$  band areas).

of diogenitic and eucritic materials that lack the 2.8  $\mu\text{m}$  signature showing that the correspondence with mineralogy is not straightforward.

Comparing the global distribution of the 2.8  $\mu\text{m}$  band with Vesta surface mineralogy (De Sanctis et al. 2012), we see that OHRT1 corresponds to a eucrite-rich howarditic composition, but other regions on Vesta with similar mineralogy (as indicated by pyroxene absorption band centers and depths) lack OH signatures. Moreover, OHRT1 broadly corresponds to the Highly Cratered Terrains 2 (HCT2), identified as the oldest Vesta surface by Marchi et al. (2012). Thus, the stronger 2.8  $\mu\text{m}$  band depths in OHRT1 could also be related to the older age of this portion of Vesta’s surface.

Comparing hydration with reflectance (McCord et al. 2012) shows that OHRT1 corresponds to a low reflectance region, suggesting that the OH-bearing material is generally darker than average Vestan materials. These data indicate a broad anti-correlation with reflectance at all scales (Figure 4(a)), but several exceptions exist, such as for the Oppia crater (OHRT2), where the 2.8  $\mu\text{m}$  band is associated with a moderate reflectance material. The association of OH with low albedo material is described by the anti-correlation between the reflectance at the 1.7  $\mu\text{m}$  and 2.8  $\mu\text{m}$  band depth (Figure 4(a)). The observations above suggest that OH on OHRT1 might be associated with dark material, possibly exogenous carbonaceous chondrites accreted from infalling primitive asteroids that are common in the main belt.

An infalling flux should produce a uniform signature of OH over the surface that is not seen on Vesta. The effect of OH accumulation due to a continuous impactor flux could locally be reset by large impacts that excavate and disperse deeper and less contaminated material. This may be the case for the relatively young Rheasilvia and Marcia craters, where we do not see the 2.8  $\mu\text{m}$  band. There are also extensive areas well outside the Rheasilvia and Marcia craters where the 2.8  $\mu\text{m}$  signature is lacking. These areas could be affected by Rheasilvia ejecta (Schenk et al. 2012; Marchi et al. 2012). Consequently, the absence of or very weak 2.8  $\mu\text{m}$  absorption in Rheasilvia, as well as in Marcia, is likely due to the resurfacing associated with impacts obscuring older regolith containing more abundant exogenous, OH-bearing material.

It must be noted, however, that these younger regions did not accumulate any detectable OH after their formation, which could argue against a temporally uniform flux of OH-bearing material such as Mighei-like carbonaceous chondrites (CM) inclusions found in howardites. They dominate by mass the meteoritic inclusions in howardites and also exhibit a significantly larger clast size with respect to inclusions of other meteorite types (Lorenz et al. 2007).

The predominance of CM inclusions is opposite to what is expected because the present impactor flux at Vesta is dominated by S-type asteroids. Using asteroid photometry from the Sloan Digital Sky Survey moving object catalog (Ivezic et al. 2001), we estimate that C-type asteroids constitute at most 10%–30% of all the present impacts at Vesta.

Moreover, CM material is more fragile than other inclusion types and to be preserved, it must be deposited on Vesta at a relatively low velocity. Furthermore, the fact that evolved minerals do not dominate the xenoliths found in HEDs also indicated that the average impact velocity at Vesta ( $5 \text{ km s}^{-1}$ ) is high enough to pulverize the impactors (Lorenz et al. 2007), suggesting that a process different from asteroid collision (Rubin & Bottke 2009) is responsible for the CM clasts.

All these observations argue against a constant flux of primitive asteroids.

An alternative hypothesis is that the OH is delivered by small CM particles up to at least centimeter size over a limited time span (cf. Rubin & Bottke 2009). This event may have delivered CM material during the early evolution of Vesta (after differentiation and crust formation), which on subsequent cratering may have mixed into the regolith. A major impact may also have produced an uneven distribution. For instance, the formation of large craters after the accretion of CM material had ceased could have resulted in a patchy distribution of OH signature.

From a dynamical standpoint, such a time-limited event may have occurred during the primordial solar system ( $\sim 10 \text{ Myr}$  after the formation of the first solids) when it is believed that the water was accreted on the Earth (Morbidelli et al. 2000; Turrini et al. 2011) or much later, during the Late Heavy Bombardment, when primitive outer solar system objects were implanted in the outer belt (Levison et al. 2009). For instance, implanted primitive

bodies in the outer main belt would have produced a significant amount of dust due to collisional grinding for several 100 Myr after the Late Heavy Bombardment (Levison et al. 2009) that may have undergone low speed accretion with Vesta (as well as on other bodies). These two possible mechanisms may also have allowed low-velocity impacts that could explain the large size of CM clasts in howardites.

Both these hypotheses represent processes that occurred before the Rheasilvia impact that has an estimated age of about 1 Gyr (Marchi et al. 2012; Schenk et al. 2012). The absence of the 2.8  $\mu\text{m}$  band in Rheasilvia could indicate that the phase of enhanced OH-delivery ended before its formation or that the age of Rheasilvia is young enough that there has not been sufficient time for buildup of a detectable quantity of carbonaceous chondrites material. Moreover, the presence of the OH band in the underlying Veneneia basin points to an impactor flux that extended after its formation. Unfortunately, Veneneia's age is not well constrained (Marchi et al. 2012; Schenk et al. 2012).

On the other hand, the occurrence of OH not associated with dark material (OVRT2) suggests that the accumulation from CM foreign materials may not account for all the OH observed and that the process of OH formation is more complex. Oppia OH deposits may have been produced by a different exogenous material delivery process (i.e., comet collision) or might have arisen from endogenous volatiles. The recent discoveries of significant amounts of volatiles in the lunar interior (Saal et al. 2008) may open new scenarios for the Vesta hydrated material origin.

The OH signature observed on Vesta shows an unexpected distribution and indicates processes that differ from those that are plausibly responsible for that signature on the Moon. The origin of most of the OH on Vesta is likely related to contamination of Vestan primordial material due to OH-bearing low-velocity impactors. This theory is consistent with evidence of CM OH-rich clast observed in the howardite meteorites. The Vestan OH distribution reveals that an important primordial process, such as the delivery of hydrated material in the main belt, may have played a role in the terrestrial planets evolution in the early stages of the solar system. This process could have also provided a way to transport organic compounds and water to main belt asteroids and terrestrial planets.

VIR is funded by the Italian Space Agency and was developed under the leadership of INAF-Istituto di Astrofisica e Planetologia Spaziali, Rome, Italy. The instrument was built by Selex-Galileo, Florence, Italy. The authors acknowledge the support of the Dawn Science, Instrument, and Operations Teams. This work was supported by the Italian Space Agency and NASA's Dawn at Vesta Participating Scientists Program. A portion of this work was performed at the Jet Propulsion Laboratory, under contract with NASA.

## REFERENCES

- Barrat, J. A., Yamaguchi, A., Bunch, T. E., et al. 2011, *Geochim. Cosmochim. Acta*, **75**, 3839
- Binzel, R. P., & Xu, S. 1993, *Science*, **260**, 186
- Cloutis, E. A., Hiroi, T., Gaffey, M. J., Alexander, C. M. O' D., & Mann, P. 2011, *Icarus*, **212**, 180
- Consolmagno, G. J., & Drake, M. J. 1977, *Geochim. Cosmochim. Acta*, **41**, 1271
- De Sanctis, M. C., Ammannito, E., Capria, M. T., et al. 2012, *Science*, **336**, 697
- De Sanctis, M. C., Ammannito, E., Migliorini, A., et al. 2011a, *MNRAS*, **412**, 2318
- De Sanctis, M. C., Coradini, A., Ammannito, E., et al. 2011b, *Space Sci. Rev.*, **163**, 329
- De Sanctis, M. C., Migliorini, A., Luzia Jasmin, F., et al. 2011c, *A&A*, **533**, A77
- Drake, M. J. 2001, *Meteorit. Planet. Sci.*, **36**, 501
- Duffard, R., Lazzaro, D., Licandro, J., et al. 2004, *Icarus*, **171**, 120
- Gaffey, M. J. 1997, *Icarus*, **127**, 130
- Gounelle, M., Zolensky, M. E., Liou, J.-C., Bland, P. A., & Alard, O. 2003, *Geochim. Cosmochim. Acta*, **67**, 507
- Hasegawa, S. M., Koji, I. M., Nonaka, H., et al. 2003, *Geophys. Res. Lett.*, **30**, 2123
- Hiroi, T., Pieters, C. M., Zolensky, M. E., & Lipschutz, M. E. 1996, *Meteorit. Planet. Sci.*, **31**, 321
- Ivezic, Z., Tabachnik, S., Rafikov, R., et al. 2001, *AJ*, **122**, 2749
- Levison, H. F., Bottke, W. F., Gounelle, M., et al. 2009, *Nature*, **460**, 364
- Lorenz, K. A., Nazarov, M. A., Kurat, G., Brandstaetter, F., & Ntaflou, Th. 2007, *Petrology*, **15**, 109
- Marchi, S., Lazzarin, M., Paolicchi, P., & Magrin, S. 2005, *Icarus*, **175**, 170
- Marchi, S., McSween, H. Y., O'Brien, D. P., et al. 2012, *Science*, **336**, 690
- McCord, T. B., Adams, J. B., & Johnson, T. V. 1970, *Science*, **168**, 1445
- McCord, T. B., Taylor, L. A., Combe, J.-P., et al. 2011, *J. Geophys. Res.*, **116**, E00G05
- McCord, T. B., et al. 2012, *Nature*, in press
- Mittlefehldt, D. W., & Lindstrom, M. M. 1997, *Geochim. Cosmochim. Acta*, **61**, 453
- Mittlefehldt, D. W., McCoy, T. J., Goodrich, C. A., & Kracher, A. 1998, *Rev. Mineral.*, **36**, 4-1
- Morbidelli, A., Chambers, J., Lunine, J. I., et al. 2000, *Meteorit. Planet. Sci.*, **35**, 1309
- Moskovitz, N. A., Willman, M., Burbine, T. H., Binzel, R. P., & Bus, S. J. 2010, *Icarus*, **208**, 773
- Pieters, C. M., Goswami, J. N., Clark, R. N., et al. 2009, *Science*, **326**, 568
- Prettyman, T. H., Mittlefehldt, D. W., Yamashita, N., et al. 2012, *Science*
- Rivkin, A. S., McFadden, L. A., Binzel, R. P., & Sykes, M. 2006, *Icarus*, **180**, 464
- Rubin, A. E., & Bottke, W. F. 2009, *Meteorit. Planet. Sci.*, **44**, 701
- Russell, C. T., & Raymond, C. A. 2011, *Space Sci. Rev.*, **163**, 3
- Russell, C. T., Raymond, C. A., Coradini, A., et al. 2012, *Science*, **336**, 684
- Saal, A. E., Hauri, E. H., Cascio, M. L., et al. 2008, *Nature*, **454**, 192
- Sato, K., Miyamoto, M., & Zolensky, M. E. 1997, *Meteorit. Planet. Sci.*, **32**, 503
- Schenk, P., O'Brien, D. P., Marchi, S., et al. 2012, *Science*, **336**, 694
- Sunshine, J. M., Farnham, T. L., Feaga, L. M., et al. 2009, *Science*, **326**, 565
- Takeda, H. 1997, *Meteorit. Planet. Sci.*, **32**, 841
- Treiman, A. H., Lanzirrotti, A., & Xirouchakis, D. 2004, *Earth Planet. Sci. Lett.*, **219**, 189
- Turrini, D., Magn, G., & Coradini, A. 2011, *MNRAS*, **413**, 2439
- Zolensky, M. E., Weisberg, M., Buchanan, P. C., & Mittlefehldt, D. W. 1996, *Meteorit. Planet. Sci.*, **31**, 518